

Article

Storage Placement and Sizing in a Distribution Grid with High PV Generation

Benjamin Matthiss ^{1,*}, Arghavan Momenifarahani ² and Jann Binder ¹

¹ Zentrum für Sonnenenergie- und Wasserstoff-Forschung Baden-Württemberg, 70563 Stuttgart, Germany; jann.binder@zsw-bw.de

² Decision Trees GmbH, 81829 München, Germany; arghavan.momenifarahani@dtrees.com

* Correspondence: benjamin.matthiss@zsw-bw.de

Abstract: With the increasing penetration of renewable resources into the low-voltage distribution grid, the demand for alternatives to grid reinforcement measures has risen. One possible solution is the use of battery systems to balance the power flow at crucial locations in the grid. Hereby, the optimal location and size of the system have to be determined in regard to investment and its effect on grid stability. In this paper, the optimal placement and sizing of battery storage systems for grid stabilization in a small low-voltage distribution grid in southern Germany with high PV penetration are investigated and compared to a grid heuristic reinforcement strategy.

Keywords: low-voltage grid; distribution grid; smart grids; power grids; energy storage; batteries; power supply; renewable energy sources; energy management



Citation: Matthiss, B.; Momenifarahani, A.; Binder, J. Storage Placement and Sizing in a Distribution Grid with High PV Generation. *Energies* **2021**, *14*, 303. <https://doi.org/10.3390/en14020303>

Received: 13 November 2020

Accepted: 31 December 2020

Published: 8 January 2021

Publisher's Note: MDPI stays neutral with regard to jurisdictional claims in published maps and institutional affiliations.



Copyright: © 2021 by the authors. Licensee MDPI, Basel, Switzerland. This article is an open access article distributed under the terms and conditions of the Creative Commons Attribution (CC BY) license (<https://creativecommons.org/licenses/by/4.0/>).

1. Introduction

The rapid increase of penetration of renewable energy resources into the distribution network can cause increased stress, especially to the low-voltage grids, such as through overvoltage situations or the exceeding of line ratings. Furthermore, the sustained need to establish a balance between energy demand and supply requires new solutions to enhance the reliable operation of the power system. Battery energy storage systems (BESSs) are being proposed as a measure to enable the integration of more renewable energy generation into the distribution grid without the need to curtail renewable generation or to reinforce the grid. The availability of storage also allows the maximization of the energy efficiency, decreases in network losses, and the ability to deliver control or reserve energy to the grid. In this paper, the optimal placement and sizing of a battery energy storage system (BESS) for grid relief in a photovoltaic (PV)-rich low-voltage distribution grid are investigated. The method used is based on a linearized load flow method and will be tested with data from a real distribution grid.

2. Literature Review

In the above-mentioned context, battery storage systems connected to distribution grids are the focus of numerous studies [1–5]. Batteries can be used to reduce distribution system losses, remove existing hindrances to the integration of renewable distributed generation, and contribute to voltage and frequency regulation [6,7] by facilitating peak shaving or decreasing the need for network expansion [8]. However, due to specific applications and operational strategies, there is a need for an appropriate procedure to size and site the mentioned systems to minimize the costs and losses [9]. Additionally, the objective function in different methodologies implies considerable variation in outcomes of the cost-optimized placement and sizing of the BESS. A network's structure, the renewable resource positions, and line-flow limits can also have impacts on optimal storage placement [10]. The mathematical problem of the optimal site and size of the storage is, in general, non-convex and high dimensional; approaches to this problem are

classified into analytic techniques, artificial intelligence techniques, classical techniques, or heuristic techniques [9,11]. Motalleb et al. proposed a heuristic method to find the optimal locations and capacity of a multi-purpose battery energy storage system (BESS) taking into account the distribution and transmission parts [12]. Fossati et al. [13] found the optimal power capacity of a BESS that minimizes the operating cost of the microgrid based on genetic methods. A fuzzy expert system determines the power delivered to or taken from the storage system. The advantage of the proposed algorithm is its easy adaptation to different types of microgrids. In [14], the economically optimal allocation of the energy storage was explored based on net present value using matrix-real-coded genetic algorithm techniques. The upside of this method is that it takes complete and overall design aspects into consideration. In [15,16], the articles give a dissertation on how to minimize the sum of operation costs and to realize the optimal site and size of the BESS based on particle swarm optimization (PSO). The objective in [17] was to enhance frequency control and reduce the operating cost by integrating a load-shedding scheme with the optimal sizing of a BESS. The results depict the better performance of frequency control based on PSO in comparison with an analytic algorithm with a load-shedding scheme. However, the issue identified in heuristic methods is that they require huge calculations, and it is uncertain if they converge to the global optimal solution. In [9], a second-order cone program (SOCP) convex relaxation of the power flow equations for optimal sizing and siting of a BESS with a lower computational burden is presented. Hereby, the objective function is formulated in two different manners: minimizing investment vs. power losses and minimizing investment vs. operational cost–benefits in a variable price market. As discussed in [18], the load and generation balancing of interconnected renewable resources and energy storage can be controlled using a dynamic energy price. The problem is formulated in a stochastic dynamic program over a finite horizon with the aim of minimizing the long-term average cost of used electricity as well as investment in storage.

3. Cost Analysis

This section follows an overview of the costs considered for battery placement and grid reinforcement. These are important for assessing the optimal placement and sizing of battery systems correctly.

3.1. Energy Storage Costs

To estimate the total costs of energy storage placement correctly, it is necessary to split the costs into power- and capacity-related costs. In [19], the relative component costs of battery storage systems were examined in a long-term storage market analysis, which was performed starting in 2014. Hereby, the total costs were split up into the cell costs, the power electronic costs, and the peripheral system costs. For residential systems, the relative costs for the power electronic components resulted in 42% of the total system costs. In this paper, it is assumed that the power electronic cost rises linearly with the rated system power of the battery. The estimated costs of the battery system were taken from [20] for the year 2019, and are shown in Table 1.

Table 1. Battery installation costs for 2019.

Type	Perc.	Costs/Value
capacity	42%	130 EUR/kwh
periphery	28%	87 EUR/kwh
power electronics	30%	93 EUR/kw
installation	-	20,000 EUR/batt
batt. lifetime	-	10 yr

3.2. Grid Reinforcement Costs

For the specific expansion costs, the two main shares for cables and installation costs are taken into account. The specific costs for the cables or lines depending on the line type are displayed in Table 2.

However, the amounts for laying the cables vary greatly, depending on the condition of the ground. For arable land, about 20,000 EUR/km can be expected, but for stony ground, the amount doubles (40,000 EUR/km). In urban areas, where roads have to be rebuilt, the costs can be raised up to 80,000 EUR/km [21]. For the installation of another cable in parallel, it is assumed that the installation costs increase by about 15% with each added line.

For the calculation of the annual costs, the useful lifespan of the lines still has to be determined. For underground cables, a lifespan of 40 years is generally assumed [22], and the normal operating life in accordance with the electricity grid charge ordinance is also 40 years [23].

Table 2. Grid reinforcement costs.

Line Type	Cost Type	Costs
0.4 kV, 4 × 50 mm	installation	60,000 EUR/km
	acquisition	3500 EUR/km
0.4 kV, 4 × 120 mm	installation	60,000 EUR/km
	acquisition	9900 EUR/km
0.4 kV, 4 × 150 mm	installation	60,000 EUR/km
	acquisition	12,000 EUR/km
parallel line installation	installation	additional 15% of installation costs
Trafo, 630 kVA	total	21,000 EUR

4. Input Data and Scenario

In this paper, real measurement data (load and irradiation) from a German distribution grid with high photovoltaic (PV) penetration were used to investigate the effects of different storage placements and grid reinforcement scenarios.

4.1. PV Generation

To establish a worst-case scenario for the grid loading induced by distributed generation, a maximum PV penetration scenario was created. Hereby, the roof area of the buildings, as well as the azimuth and tilt angles, was estimated to calculate the in-plane irradiance. It was assumed that the usable roof area for PV installations is an 80% share of the total roof area. With this information and the knowledge about the module size and type, an estimate of the maximum possible PV capacity is established. This scenario is called $P_{PV, max}$. To model the PV generation within the network, the Python library PVLIB [24] is used. This package includes all necessary functions for modeling the complete chain from the measured irradiance to the inverter AC output power. To model the diffuse irradiation, the Perez model was used. The irradiance levels of global horizontal irradiation (GHI) and diffuse horizontal irradiation (DHI) were measured locally within the distribution grid.

4.2. Simulation Scenario

Because of the computational complexity of the problem (distribution grid with 106 nodes), it is not possible to optimize in a single shot over one year. To capture the major grid stress for the battery placement, a worst-case period was selected from the measured data. The costs were analyzed over one year. The selected time span was three days long, and showed the highest consecutive net load (generation minus load) of the whole dataset.

Different simulation scenarios were created to evaluate the dependency on voltage limitation and PV penetration. The selected PV penetrations are 50% and 80% relative

to $P_{PV, \max}$. The maximum allowed voltage deviations are 3% and 5% from the nominal voltage. In Figure 1, the resulting voltage distribution for the selected worst-case period with an 80% PV penetration is displayed.

4.3. Battery Sizing and Placement

The objective of the algorithm is the optimized placement of battery storage systems in order to balance voltage violations within the low-voltage distribution grid. The goal is hereby to minimize the installation costs based on Table 1 under the constraints that all grid limits are within their operational limits.

The algorithm is based on a linearized load-flow method presented in [25] and the optimization framework that is used in [26]. The resulting optimization problem is solved via successive linear programming (SLP). The battery system can be simulated with a fixed efficiency. The voltage drops within the distribution grid are calculated using the linearized load-flow algorithm mentioned above. The time resolution of the algorithm is 1 h. This can be justified with the properties of the battery system: The battery capacity is larger than the 1 h times the maximum rated power of the battery. Furthermore, the reaction time of the battery is very fast. Therefore, the battery can compensate for the fluctuations within this hour, and the average power over this time span can be used for the sizing of the battery. This, however, slightly underestimates the power values and, therefore, also the costs for the power electronics.

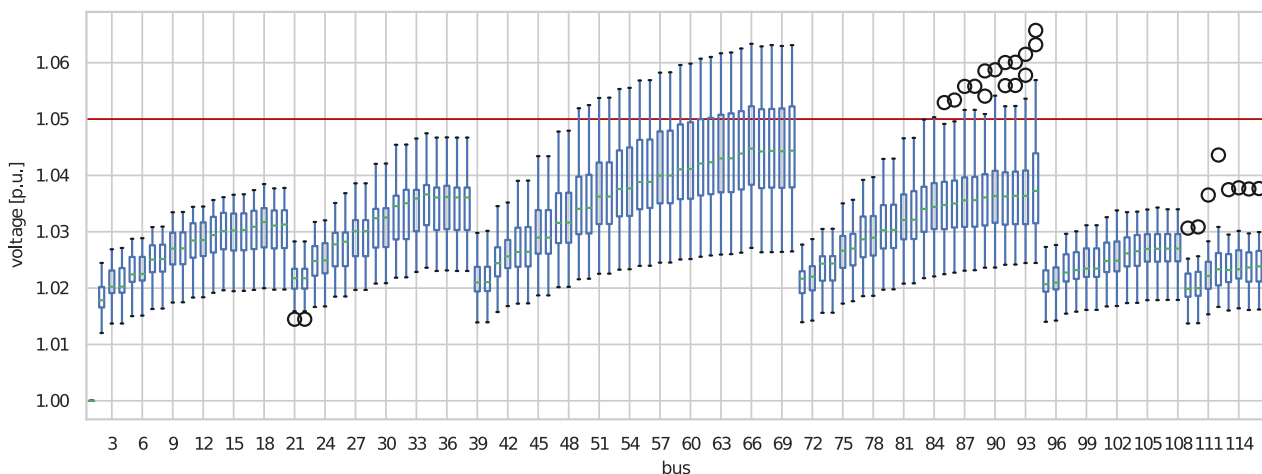


Figure 1. Voltage distribution for the selected worst-case scenario without battery or energy curtailment. The voltage limit is 1.05 p.u., which is clearly exceeded.

5. Approach

In this section, we will briefly describe the methods we used for the automated grid reinforcement and the battery placement algorithm. As the specific goal of the paper is to compare the optimal battery placement with grid reinforcement, alternatives, such as curtailment of renewable generation to relax the grid stress, are not taken into account.

5.1. Grid Reinforcement

The necessary grid reinforcement to meet the voltage constraints was calculated with a heuristic approach. Hereby, the critical nodes of each branch were identified, and the grid was reinforced until the given voltage limits were met at the corresponding nodes. The procedure of the algorithm is shown in Figure 2. The algorithm always chooses the cheapest option for the reinforcement based on the costs shown in Table 2. Hereby, whether it is cheaper to install multiple smaller lines in parallel or to install a larger line was also evaluated.

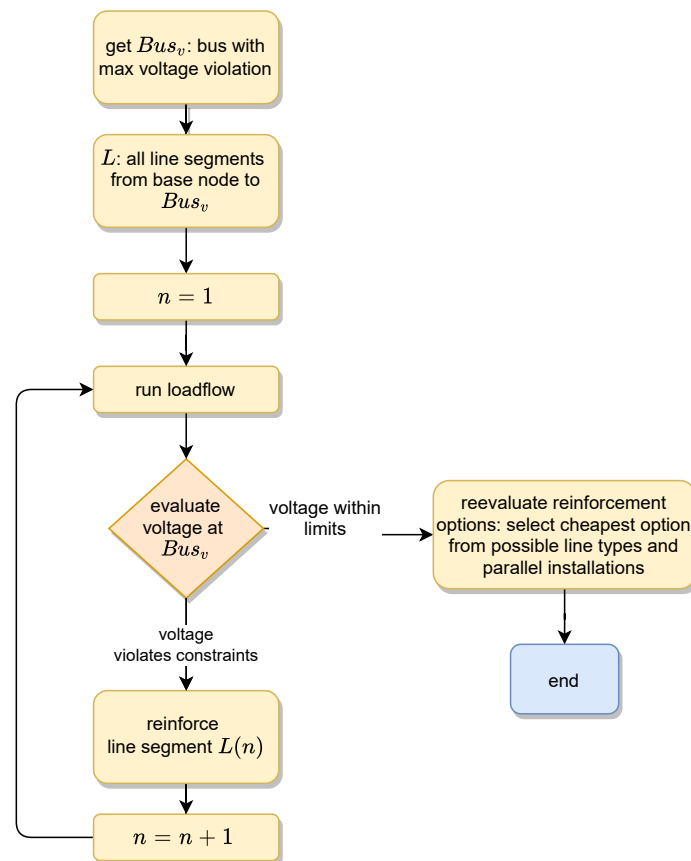


Figure 2. Flowchart of the heuristic grid reinforcement algorithm. The method shown above was repeated for all branches.

As mentioned before, the simulation period is three days. Therefore, multiple charging cycles are captured. This implies that the possibility to discharge the battery before the next cycle is ensured by the algorithm. Otherwise, the optimal size of the battery cannot be calculated correctly.

The optimization places the battery storage units based on the costs shown in Table 1 and, at the same time, calculates an optimized charge trajectory for the batteries. Furthermore, constraints can be included, e.g., the number of batteries that the algorithm is allowed to place.

This can be shown by an example calculation: In Figure 1, the voltage situation within the grid is shown for a day with high solar PV generation and without an installed battery or curtailment of PV generation. The voltage limit within the grid is 1.05 p.u., which is surpassed in two branches here. In Figure 3, the voltage distribution with the use of the optimized operation of one battery and curtailment is shown: The voltage limits are obeyed at all times. The algorithm chose to place the battery at bus 65 with a size of 83 kWh. The size was determined with the help of the provided irradiation and load profiles.

In this section, the results of the above-mentioned algorithms in the given simulation scenario are shown and evaluated.

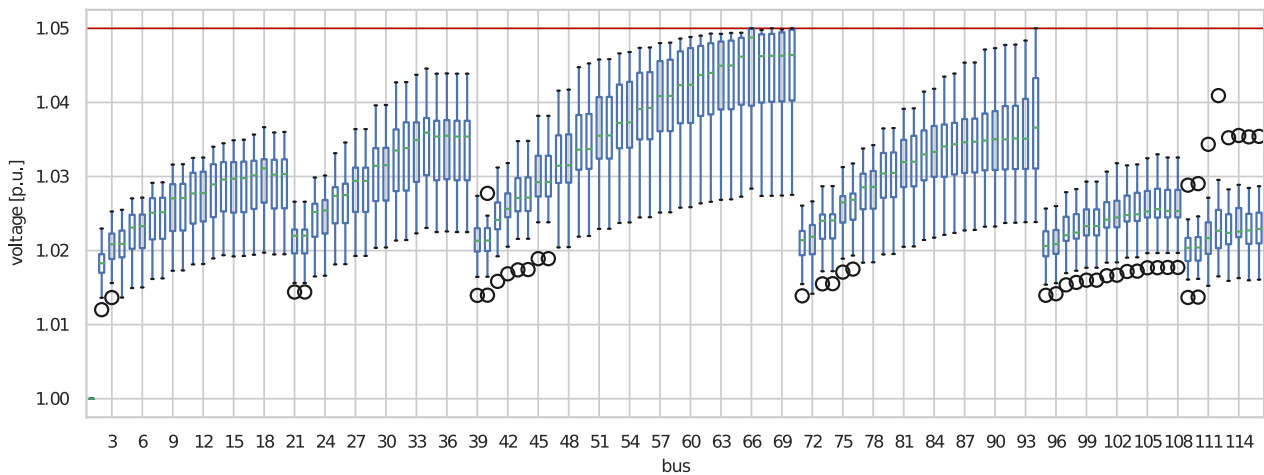


Figure 3. Voltage distribution for a day with high solar photovoltaic (PV) generation and one installed battery. In this case, the voltage limit is obeyed at all nodes. The algorithm selected a battery placement at buses 65 and 93 to avoid voltage limit violations. Whiskers were set to $1.5 \times \text{IQR}$, the circles represent data points exceeding that range.

5.2. Grid Reinforcement

The grid reinforcement algorithm has been shown to be computationally effective and, at the same time, sufficient for fulfilling the task of calculating a cost-effective grid reinforcement. As it is a heuristic algorithm, the global optimality of the solution cannot be guaranteed. For radial distribution grids, however, a high-quality solution can be assumed. In Figure 4b, a comparison of the bus voltages of the original grid and the reinforced one is displayed. It can be seen that the algorithm added additional elements to reinforce the grid until the voltage limits were met at all nodes. The resulting reinforcement is shown in Figure 4a. The red edges of the graph indicate the reinforced line segments. Only the line segments with voltage problems were reinforced—in this case, three branches.

The selection of the line types depends on the amount of reinforcement needed to meet the voltage constraints. In this example, the algorithm chose to use a cable of the type NAYY 4×120 SE 18 times and the smaller NAYY 4×50 SE three times (see Table 3). As the transformer loading was still within the limits, it was not replaced or reinforced.

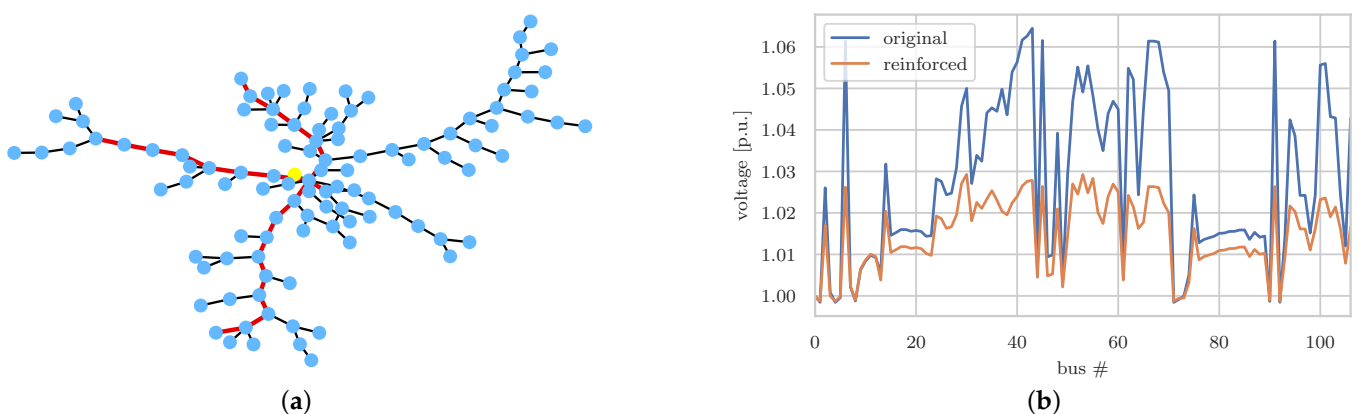


Figure 4. Exemplary results from the automated grid reinforcement algorithm. On the left, a graph with the reinforced line segments is shown. The yellow node indicates the transformer and the red edges indicate reinforced line segments. A comparison of the resulting bus voltages is shown on the right. In this case, a voltage limit of 1.03 p.u. was used. (a) Graph diagram of the reinforced grid; (b) Voltage comparison of the reinforced grid.

Table 3. Example result of the grid reinforcement algorithm: overview of the installed assets and costs.

From Bus	To Bus	n Parallel	Type	Cost [k€]
1	105	2	NAYY 4 × 120 SE	109.5
1	73	2	NAYY 4 × 120 SE	109.5
1	106	3	NAYY 4 × 120 SE	131.1
2	28	1	NAYY 4 × 120 SE	87.9
2	104	2	NAYY 4 × 120 SE	109.5
3	61	1	NAYY 4 × 120 SE	87.9
3	73	2	NAYY 4 × 120 SE	109.5
6	43	1	NAYY 4 × 50 SE	81.5
6	68	2	NAYY 4 × 120 SE	109.5
28	29	1	NAYY 4 × 50 SE	81.5
29	30	1	NAYY 4 × 50 SE	81.5
50	57	1	NAYY 4 × 120 SE	87.9
50	61	1	NAYY 4 × 120 SE	87.9
56	57	1	NAYY 4 × 120 SE	87.9
63	70	2	NAYY 4 × 120 SE	109.5
63	69	2	NAYY 4 × 120 SE	109.5
65	70	2	NAYY 4 × 120 SE	109.5
65	106	1	NAYY 4 × 120 SE	87.9
68	100	2	NAYY 4 × 120 SE	109.5
69	100	2	NAYY 4 × 120 SE	109.5
104	105	2	NAYY 4 × 120 SE	109.5

5.3. Battery Placement

The results of the battery placement are summed up in Table 4 for the different scenarios. For the scenario of a 50% penetration and a maximum voltage deviation of 5% relative to V_{nom} , no battery placement is needed. If the maximum voltage deviation is decreased to 3%, two batteries have to be placed. For the scenario with 80% PV penetration, there is a maximum voltage deviation of 5% relative to V_{nom} and the locations of the batteries stay almost the same as before, but the sizes increase. If the maximum voltage deviation is decreased to 3% in this case, a third battery has to be added. The results are additionally shown in Figure 5a,b. Here, the placements for the 80% PV penetration and both voltage limitations are shown in a graph.

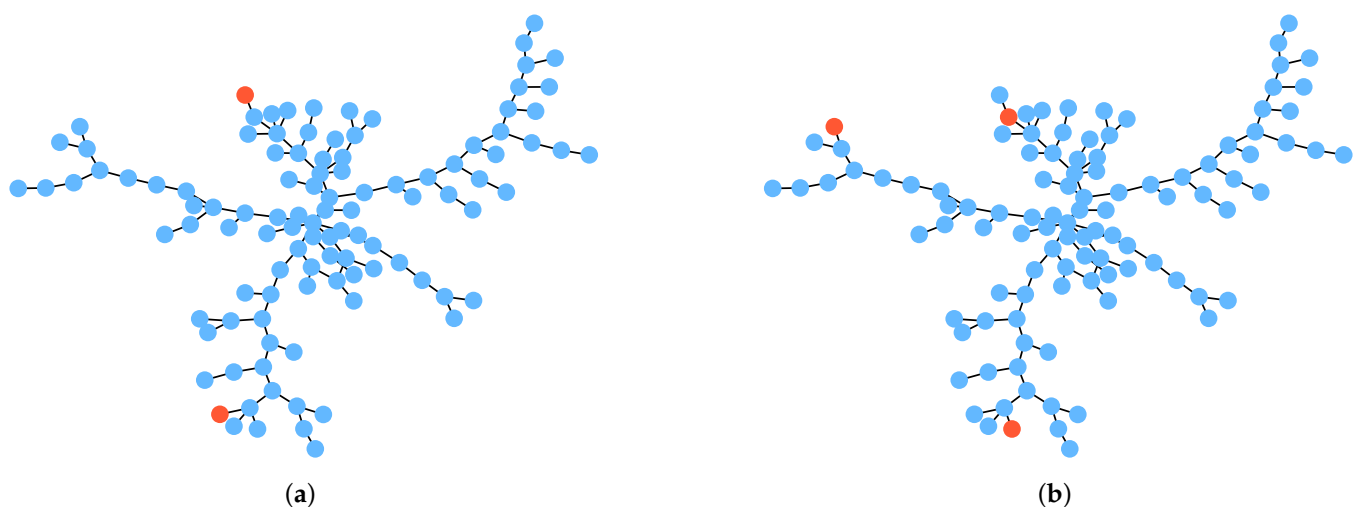


Figure 5. Optimal battery placement for voltage stability within the test grid. (a) 50% PV penetration, voltage limit 3%. (b) 80% PV penetration, voltage limit 3%.

Table 4. Size, maximum power, and location of the batteries.

PV Pen. [$P_{PV, \max}$]	ΔV_{\max} [V_{nom}]	Batt. 1			Batt. 2			Batt. 3		
		C [kWh]	P [kW]	Bus #	C [kWh]	P [kW]	Bus #	C [kWh]	P [kW]	Bus #
50 %	5 %	-	-	-	-	-	-	-	-	-
	3 %	61	15	30	99	20	42	-	-	-
80 %	5 %	75	20	30	149	30	43	-	-	-
	3 %	377	61	29	414	67	45	909	25	59

In all cases, the placement of the battery varies just slightly by one or two buses. This indicates that the solution surface is relatively flat with respect to the battery position in the grid.

5.4. Comparison

In this section, the results of the battery placement and the grid reinforcement algorithm will be compared. In contrast to the previous section, Section 5.3, some constraints on the number of batteries to place are added to investigate the sensitivity on the number of batteries installed. Therefore, two additional scenarios are introduced: one where the number of batteries is fixed to 5 and one with 10 batteries.

The results regarding the absolute investment costs are shown in Table 5. The cheapest solution for the given scenarios is the installation of batteries to maintain the grid voltage stability. The costs increase with additional batteries, although the individual size of the batteries decreases. The most expensive option regarding the investment costs is grid reinforcement.

Table 5. Investment cost comparison.

PV Pen. [$P_{PV, \max}$]	ΔV_{\max} [V_{nom}]	Grid Reinf.	5 Batt.	10 Batt.	Unconstrained	
		[k€]	[k€]	[k€]	[k€]	[n batt.]
50 %	3%	710	138	238	79	2
	5%	-	-	-	-	-
80 %	3%	1679	307	406	273	3
	5%	488	154	254	94	2

A more interesting comparison is that of the yearly costs. In this case, the maintenance costs for the battery as well as the grid are neglected, as they vary greatly. As mentioned before, the lifetime for the battery is assumed to be 10 years, and the lifetime for the cables is assumed to be 40 years. The results of this comparison are shown in Table 6. The result is similar to that of the investment costs, although the difference between the battery placement and the grid reinforcement is less pronounced. However, in all cases, the installation of batteries is cheaper than the grid reinforcement.

Table 6. Yearly cost comparison (assumed lifetime: battery = 10 y, cable = 40 y).

PV Pen. [$P_{PV, \max}$]	ΔV_{\max} [V_{nom}]	Grid Reinf.	5 Batt.	10 Batt.	Unconstrained	
		[k€]	[k€]	[k€]	[k€]	[n batt.]
50%	3%	18	14	24	8	2
	5%	0	0	0	0	0
80%	3%	42	31	41	27	3
	5%	12	15	25	9	2

6. Conclusions and Outlook

In this paper, the study case of a low-voltage distribution grid with high PV potential and solutions to avoid the resulting grid violations were presented. Hereby, two algorithms were compared: one for the automated placement and sizing of battery storage systems within a distribution grid, and another algorithm for automated grid reinforcements. Both algorithms have been shown to work, fulfill their tasks, and avoid grid overloading for the suggested implementations. These algorithms will be used to evaluate the possible solutions for various distribution grids with congestion problems.

In the presented case, the use of well-placed batteries could reduce grid strain and be more cost effective compared to grid reinforcement measures. Further benefits, such as higher local consumption, have not yet been examined. The results presented in this paper, however, are only valid for the given scenario—the presented distribution grid and the assumed costs for battery installation and grid reinforcement. Furthermore, other solutions, such as tap-changing transformers or curtailment, were not considered within this paper.

However, the algorithm is capable of incorporating additional congestion management options, such as the curtailment of renewable generation, load shifting, etc. These possibilities will be examined in a future paper.

Author Contributions: Conceptualization, B.M.; methodology, B.M.; software, B.M.; validation, B.M. and A.M.; resources, B.M. and J.B.; writing—original draft preparation, B.M. and A.M.; visualization, B.M.; project administration, B.M. and J.B.; funding acquisition, B.M. and J.B. All authors have read and agreed to the published version of the manuscript.

Funding: This work was funded by the Federal Ministry of Economy and Energy in Germany as part of the research project “NemoGrid” (FKZ 0350016A). The authors gratefully acknowledge this support. They are solely responsible for the contents of this publication.

Institutional Review Board Statement: Not applicable.

Informed Consent Statement: Not applicable.

Conflicts of Interest: The authors declare no conflict of interest.

References

1. Dunn, B.; Kamath, H.; Tarascon, J.M. Electrical Energy Storage for the Grid: A Battery of Choices. *Science* **2011**, *334*, 928–935. [[CrossRef](#)] [[PubMed](#)]
2. Divya, K.; Østergaard, J. Battery Energy Storage Technology for Power Systems—An Overview. *Electr. Power Syst. Res.* **2009**, *79*, 511–520. [[CrossRef](#)]
3. Beaudin, M.; Zareipour, H.; Schellenberglobe, A.; Rosehart, W. Energy Storage for Mitigating the Variability of Renewable Electricity Sources: An Updated Review. *Energy Sustain. Dev.* **2010**, *14*, 302–314. [[CrossRef](#)]
4. Ferreira, H.L.; Garde, R.; Fulli, G.; Kling, W.; Lopes, J.P. Characterisation of Electrical Energy Storage Technologies. *Energy* **2013**, *53*, 288–298. [[CrossRef](#)]
5. Mateo, C.; Sánchez, Á.; Frías, P.; Rodríguez-Calvo, A.; Reneses, J. Cost–Benefit Analysis of Battery Storage in Medium-Voltage Distribution Networks. *IET Gener. Transm. Distrib.* **2016**, *10*, 815–821. [[CrossRef](#)]
6. Oudalov, A.; Chartouni, D.; Ohler, C. Optimizing a Battery Energy Storage System for Primary Frequency Control. *IEEE Trans. Power Syst.* **2007**, *22*, 1259–1266. [[CrossRef](#)]
7. Aditya, S.; Das, D. Battery Energy Storage for Load Frequency Control of an Interconnected Power System. *Electr. Power Syst. Res.* **2001**, *58*, 179–185. [[CrossRef](#)]
8. Lazzaroni, P.; Repetto, M. Optimal Planning of Battery Systems for Power Losses Reduction in Distribution Grids. *Electr. Power Syst. Res.* **2019**, *167*, 94–112. [[CrossRef](#)]
9. Grover-Silva, E.; Girard, R.; Kariniotakis, G. Optimal Sizing and Placement of Distribution Grid Connected Battery Systems through an SOCP Optimal Power Flow Algorithm. *Appl. Energy* **2018**, *219*, 385–393. [[CrossRef](#)]
10. Bose, S.; Gayme, D.F.; Topcu, U.; Chandy, K.M. Optimal Placement of Energy Storage in the Grid. In Proceedings of the 2012 IEEE 51st IEEE Conference on Decision and Control (CDC), Maui, HI, USA, 10–13 December 2012; pp. 5605–5612. [[CrossRef](#)]
11. Prakash, P.; Khatod, D.K. Optimal Sizing and Siting Techniques for Distributed Generation in Distribution Systems: A Review. *Renew. Sustain. Energy Rev.* **2016**, *57*, 111–130. [[CrossRef](#)]
12. Motalleb, M.; Reihani, E.; Ghorbani, R. Optimal Placement and Sizing of the Storage Supporting Transmission and Distribution Networks. *Renew. Energy* **2016**, *94*, 651–659. [[CrossRef](#)]

13. Fossati, J.P.; Galarza, A.; Martín-Villate, A.; Fontán, L. A Method for Optimal Sizing Energy Storage Systems for Microgrids. *Renew. Energy* **2015**, *77*, 539–549. [[CrossRef](#)]
14. Chen, C.; Duan, S.; Cai, T.; Liu, B.; Hu, G. Optimal Allocation and Economic Analysis of Energy Storage System in Microgrids. *IEEE Trans. Power Electron.* **2011**, *26*, 2762–2773. [[CrossRef](#)]
15. Arabali, A.; Ghofrani, M.; Etezadi-Amoli, M. Cost Analysis of a Power System Using Probabilistic Optimal Power Flow with Energy Storage Integration and Wind Generation. *Int. J. Electr. Power Energy Syst.* **2013**, *53*, 832–841. [[CrossRef](#)]
16. Ahmadian, A.; Sedghi, M.; Aliakbar-Golkar, M.; Elkamel, A.; Fowler, M. Optimal Probabilistic Based Storage Planning in Tap-Changer Equipped Distribution Network Including PEVs, Capacitor Banks and WDGs: A Case Study for Iran. *Energy* **2016**, *112*, 984–997. [[CrossRef](#)]
17. Kerdphol, T.; Qudaih, Y.; Mitani, Y. Battery Energy Storage System Size Optimization in Microgrid Using Particle Swarm Optimization. In Proceedings of the IEEE PES Innovative Smart Grid Technologies Europe, Istanbul, Turkey, 12–15 October 2014, pp. 1–6. [[CrossRef](#)]
18. Harsha, P.; Dahleh, M. Optimal Management and Sizing of Energy Storage Under Dynamic Pricing for the Efficient Integration of Renewable Energy. *IEEE Trans. Power Syst.* **2015**, *30*, 1164–1181. [[CrossRef](#)]
19. Müller, M.; Viernstein, L.; Truong, C.N.; Eiting, A.; Hesse, H.C.; Witzmann, R.; Jossen, A. Evaluation of Grid-Level Adaptability for Stationary Battery Energy Storage System Applications in Europe. *J. Energy Storage* **2017**, *9*, 1–11. [[CrossRef](#)]
20. Bansal, V. Building A Bankable Solar + Energy Storage Project. Available online: https://16iwyl195vfvgoqu3136p2ly-wpengine.netdna-ssl.com/wp-content/uploads/2018/10/PV-Magazine-Webinar_11-Oct-2018_Sterling-and-Wilson.pdf (accessed on 3 May 2019).
21. Rupp, L.; Brunner, M.; Tenbohlen, S. Einfluss Dezentraler Wärmepumpen auf die Netzausbaukosten des Niederspannungsnetzes; In Proceedings of the Power and Energy Student Summit (PESS) 2015, Dortmund, Germany, 13–14 Januar 2015. [[CrossRef](#)]
22. Hofman, O. Vergleich Erdkabel–Freileitung Im 110-kV-Hochspannungsbereich. Technical Report. 2010. Available online: <https://www.yumpu.com/de/document/view/45325316/vergleich-erdkabel-freileitung-im-110-kv-hochspannungsbereich> (accessed on 29 April 2019).
23. Heuck, K.; Dettmann, K.D.; Schulz, D. *Elektrische Energieversorgung Erzeugung, Übertragung und Verteilung elektrischer Energie für Studium und Praxis*; Vieweg+Teubner: Wiesbaden, Germany, 2010.
24. Holmgren, W.F.; Hansen, C.W.; Mikofski, M.A. Pvlb Python: A Python Package for Modeling Solar Energy Systems. *J. Open Source Softw.* **2018**, *3*, 884. [[CrossRef](#)]
25. Matthiss, B.; Kraft, M.; Binder, J. Fast Probabilistic Load Flow for Non-Radial Distribution Grids. In Proceedings of the 2018 IEEE International Conference on Environment and Electrical Engineering and 2018 IEEE Industrial and Commercial Power Systems Europe (EEEIC / I CPS Europe), Palermo, Italy, 12–15 June 2018; pp. 1–6. [[CrossRef](#)]
26. Matthiss, B.; Momenifarhani, A.; Ohnmeiss, K.; Felder, M. Influence of Demand and Generation Uncertainty on the Operational Efficiency of Smart Grids. *arXiv* **2018**, arXiv:cs/1812.01886.